

Rational design, molecular characterization and dissociation mechanisms of PROTACs targeting hFAAH

Yuxin Xiao^{1#}, Na Li^{2#}, Dazhi Cheng¹, Yan Cheng², Huaichuan Duan², Yuting Song², Xinmin Wang², Zuoxin Ou¹, Ting Luo², Hubing Shi^{2*}, Jianping Hu^{1*}

¹ Key Laboratory of Medicinal and Edible Plants Resources Development of Sichuan Education Department, School of Pharmacy, Chengdu University, Chengdu, China.

² Institute of Breast Health Medicine, State Key Laboratory of Biotherapy, West China Hospital, Sichuan University and Collaborative Innovation Center, Chengdu, China.

[#] These authors contributed equally to this work.

* For correspondence: Hubing Shi, shihb@scu.edu.cn; Jianping Hu, hjpgcdu@163.com

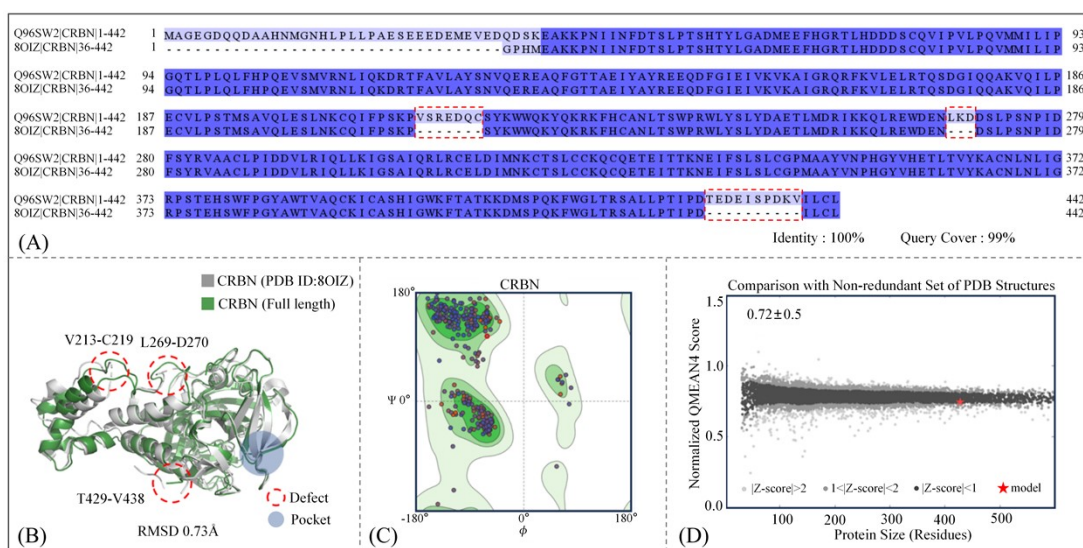


Figure S1. Residue complementation and structural rationalization validation for CRBN. (A) The sequence of CRBN (PDB ID: 8OIZ) was aligned against the UniProt entry Q96SW2; (B) superimposition of CRBN crystal structure with the template protein, respectively shown in green and gray; ramachandran plot (C) and QMEAN Z-score distribution (D) for the completed CRBN structure.

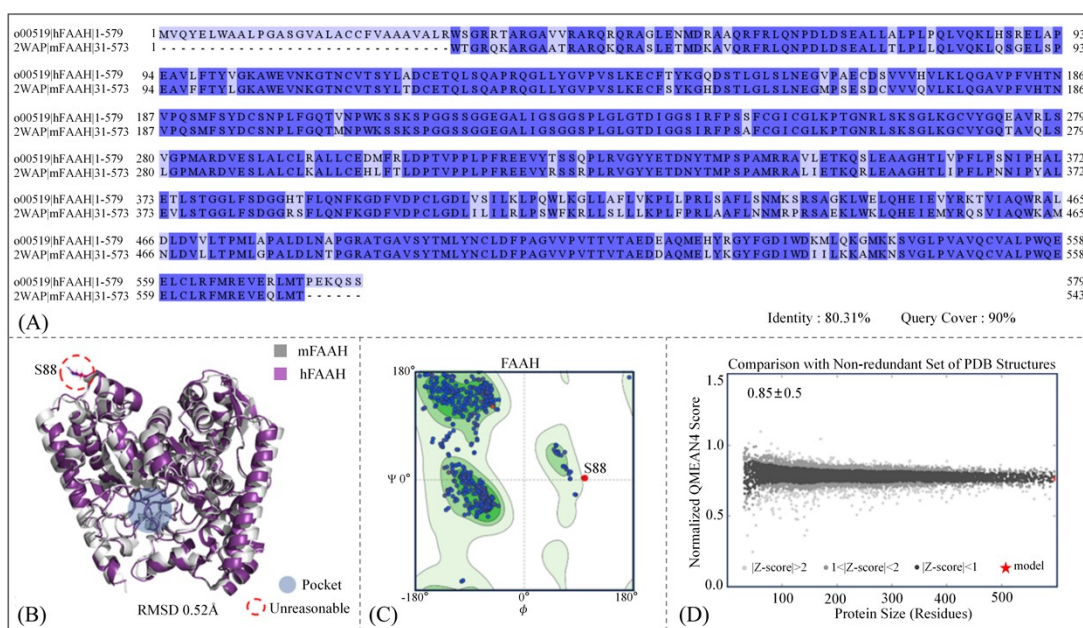
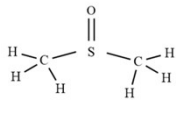
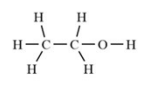


Figure S2. Homology modeling and structural rationalization verification for hFAAH. (A) Sequence alignment between mouse mFAAH (PDB ID: 2WAP) and human hFAAH (UniProt entry: O00519); (B) superimposition of the template mFAAH and the modeled hFAAH, respectively shown in purple and gray; Ramachandran plot (C) and QMEAN Z-score distribution (D) for the modeled hFAAH structure.

Table S1: Amber ff99SB force field parameters for the cosolvents used.

Solvent name and formula	Atom name	atom type	Charge
DMSO - Dimethyl sulfoxide 	C1	CT	-0.0354
	C2	CT	-0.0354
	S	S	+0.1317
	O1	OS	-0.4281
	H1	HC	+0.0612
	H2	HC	+0.0612
	H3	HC	+0.0612
	H4	HC	+0.0612
	H5	HC	+0.0612
	H6	HC	+0.0612
	EtOH - Ethanol 	C1	CT
C2		CT	+0.5193
O1		OH	-0.7114
H1		HO	+0.4147
H2		HI	-0.0822
H3		HI	-0.0822
H4		HC	+0.0640
H5		HC	+0.0640
H6		HC	+0.0640

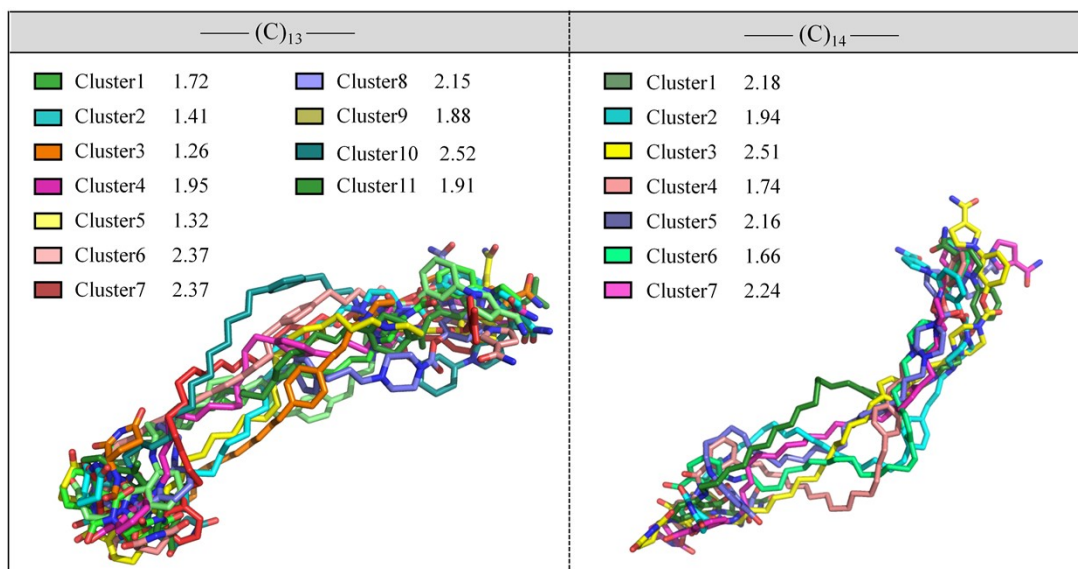


Figure S3. The representative conformational clusters and their minimum core RMSD values

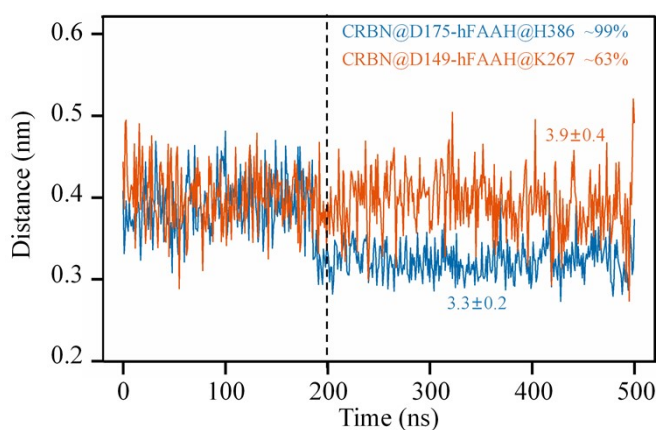


Figure S4. Time evolution of the salt-bridge distance between hFAAH and CRBN in two systems

Table S2: Statistics on interfacial water

Interface statistic	hFAAH_CRB	hFAAH_C13p_CRB
	N	N
Interface area BSA (\AA^2)	808 ± 276	1056 ± 301
Number of interface water ^a		
Range	3-19	4-23
Mean	11.0	12.9
Per 1000 \AA^2 of BSA	13.6	12.2
Number of water mediated H-bonds ^b		
Range	5-27	8-26
Mean	10.3	14.1
Per 1000 \AA^2 of BSA	12.7	13.4
Number of bridging water molecules ^c		
Range	0-11	0-15
Mean	3.2	5.2
Per 1000 \AA^2 of BSA	4.0	4.9

^aWater molecules ≤ 4.5 \AA from interface atoms of both the subunits.

^bH-bonds between interface waters and interface protein atoms.

^cInterface waters making H-bonds with both interacting subunits

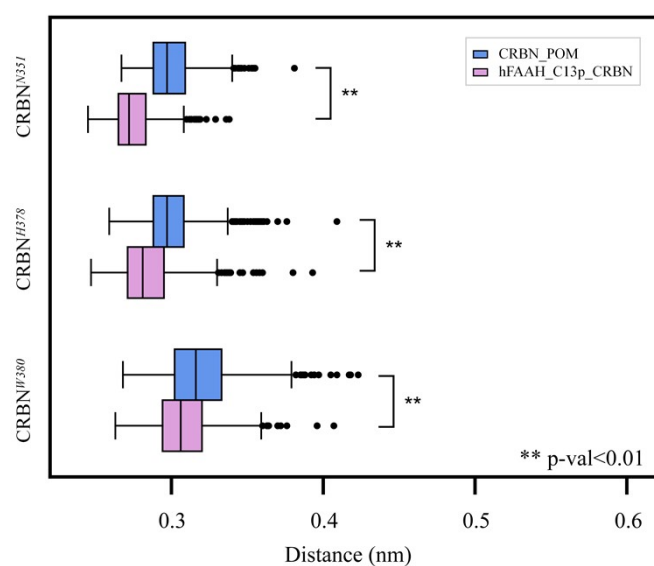


Figure S5. Distance distributions of the three key H-bonds in CRBN_POM and hFAAH_C13p_CRBN. The data were obtained from the equilibrium stage (200–500 ns) of cMD simulations for each system; Welch's t-test indicates that the differences are statistically significant.

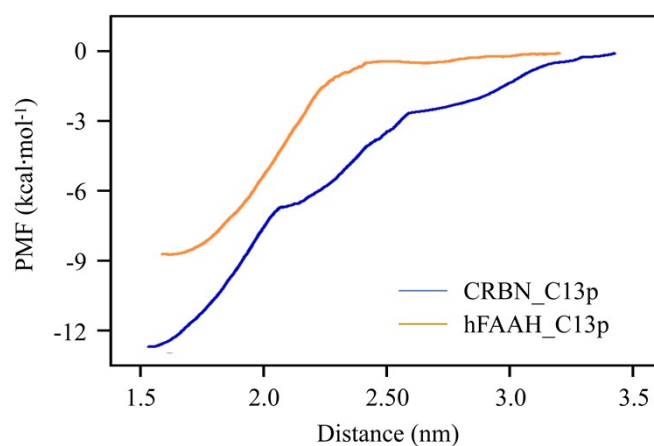


Figure S6. PMF curves for the dissociation of C13p from the CRBN_C13p and hFAAH_C13p systems.

